인이 함유된 EDTA-Co 구조 제조 및 전기화학적 촉매로서 산소 환원 반응 적용 시 상승효과

김관우 · Jinglei Yang*,† · 김주헌†

중앙대학교 공과대학 화학신소재공학부, *홍콩과학기술대학교 기계 & 항공우주공학과

(2019년 8월 20일 접수, 2019년 10월 1일 수정, 2019년 10월 2일 채택)

Synthesis of P Doped EDTA-Co Structure and Synergistic Effect of ORR as Electrochemical Catalyst

Kwanwoo Kim, Jinglei Yang*,†, and Jooheon Kim†

School of Chemical Engineering & Materials Science, Chung-Ang University, Seoul 06971, Korea
*Department of Mechanical and Aerospace Engineering, The Hong Kong University of Science and Technology, Hong Kong
(Received August 20, 2019; Revised October 1, 2019; Accepted October 2, 2019)

초록: 이번 연구를 통해서 이전에 보고되지 않은 구조를 가진 전기화학 음극 촉매를 성공적으로 개발했다. 이는 EDTA와 Co의 결합에 P를 도핑함으로써 제작되었다. EDTA는 6개의 리간드 부위를 통하여 전이금속과 6개의 배위 결합을 진행하여 팔면체의 구조를 형성한다. 또한 헤테로 원자를 도핑함으로써, 촉매 표면의 원자 및 스핀전하 밀도를 변화시켜 산소의 흡착에너지를 낮추어 산소환원반응에 보다 유리하게 변화시켜 촉매의 특성을 향상시킨다. 성공적인 촉매를 합성하기 위해 간단한 1단계 열분해 반응을 통하여 Co 및 P를 EDTA와 합성하였으며, 그 결과 Co 및 P의 첨가로 인해 전기화학적 특성의 증가가 증명되었다. 또한 이 연구는 단순히 Co와 P가 각각 더해지는 효과 그 이상의 상승효과를 보였다.

Abstract: In this study, we successfully developed an electrochemical cathodic catalyst with a previously unreported structure. In essence, a new material was fabricated by doping EDTA-Co with P. EDTA has six ligand sites and forms an octahedral structure through six coordination bonds with transition metals. In addition, by doping hetero atoms, the atomic and spin charge density of the catalyst surface are changed to lower the adsorption energy of oxygen, which leads to more favorable reactions and enhances the catalytic properties. Co and P were added to EDTA to synthesize a successful catalyst, and testing confirmed an increase in electrochemical performance due to the addition of Co and P. Moreover, this work demonstrates that the synergy effect exceeds that of simply adding Co and P.

Keywords: oxygen reduction reaction (ORR), ethylenediaminetetraacetic acid (EDTA), phosphorus (P) doping microporous carbon, high specific surface area, six coordination between Co and EDTA.

Introduction

Due to the continuously increasing energy consumption and depletion of environmentally harmful fossil fuels, the development of eco-friendly and renewable energy is attracting significant attention from the scientific research community.[1] Among the various energy storage media options, metal-air batteries have high energy storage density and theoretically have an air electrode serving as the cathode electrode, which allows an infinite supply of resources. In addition, metal-air batteries have the advantage of being very similar in structure and function to the widely used Li-ion battery, which eliminates any large changes in energy storage industrial processing.[2-4]

The electrochemical performance of a metal-air battery is determined by its reactivity with oxygen in the air electrode's cathode. The more oxygen that is adsorbed and desorbed on the electrode's surface, the more electric charge that gets gen-

†To whom correspondence should be addressed.
jooheonkim@cau.ac.kr, ORCID 0000-0002-6644-7791
ooxxx223@gmail.com, ORCID 0000-0002-9413-9016

erated, and the higher the energy storage density. Therefore, in order to obtain a metal-air battery with high energy storage density, the cathode electrode's oxygen reactivity must be elevated.[5,6] However, this poses a challenge, as the cathode has a very low reactivity with oxygen, and thus requires a catalyst material to increase the reactivity. Various studies have been conducted to determine the optimal electrochemical catalyst required at the cathode. Several studies have shown Pt/C to be the best performing catalyst.[7] However, on account of Pt/C has resource scarcity and high cost, carbon-based materials have been studied as alternatives, due to their low cost and specialized properties. However, the catalyst composed only of carbon has low reactivity with oxygen and is low in efficiency as an electrochemical catalyst. In order to overcome this, doping with hetero atom (B, N, S, P) improves performance.[8,9] Moreover, synergistic effects are produced through bonding with metals.[10]

Many previous studies have conducted material-based experiments that consist only of carbon such as carbon nanotube (CNT) and graphene. In this study, however, ethylenediaminetetraacetic acid (EDTA) was selected as the carbon-based catalyst material. EDTA contains two amine-like structures that contain N. This has the advantage of having pyridinic N, pyrrolic N, graphitic N and oxidized N structures of N-doped material even without N doping. EDTA has six ligand functional groups; when it encounters transition metals, it undergoes coordination bonding to form octahedral structures.[11,12] Throughout this process, the EDTA maintains a porous texture and high surface area, which is highly advantageous for an electrochemical catalyst. The electrolyte and air move between the pores and the coexistence of all three-phases (gas-liquid-solid) increases oxygen reactivity and provides a smooth passage for charge transfer.[13,14] In this work, we report the development of a novel electrochemical catalyst through the combination of EDTA and cobalt (Co), a member of the transition metal family. Furthermore, the addition of P generates supplemental synergistic effects that demonstrates the efficacy of our EDTA-Co and P catalyst[15]— a solution, that to the best of our knowledge, has yet to be proposed.

Experimental

Synthesis of EDTA-Co Bond Precursor. All reagents were used without further purification. 1.6 g of EDTA ($\geq$ 99%, Sigma-Aldrich) was added to 20 mL of DI water and stirred for 2 h. Next, the solution was ultrasonicated and dispersed for

4 h (VCX-750, Ultrasonic Processor) using a 750 W output. 0.3 g of Co(Cl)$_2$·6H$_2$O (97%, Deajung Chemical Co., Korea) was added to the dispersed EDTA solution to induce bonding between the EDTA and Co constituents. Finally, the solution was stirred for 20 min and allowed to stand for 2 h until bonding completed. The EDTA-Co bonded precursor was obtained after washing and filtering with DI water.

Synthesis of Porous Electrocatalytic Samples. 1.6 g of EDTA or EDTA-Co, 0.8 g of triphenylphospine ($\geq$95%, Sigma-Aldrich) 0.8 g of potassium hydroxide (85%, Sigma-Aldrich), and 0.8 g of melamine (99%, Deajung Chemical Co., Korea) were mixed in a mortar until it transformed into a semi-solid state with an adhesive-like viscosity. The resulting mixture was transferred to an alumina boat and calcined at a heating rate of 10 °C/min to 750 °C for 2 h under N$_2$ flow. After the sample cooled, it was refluxed in 200 mL of 0.1 M sulfuric acid (H$_2$SO$_4$, 0.1 N Standard Solution, Alfa-Aesar) at 80 °C for 12 h to remove impurities. Afterwards, the products were washed with DI water and ethanol, filtered, and dried overnight in a 70 °C oven. Using this experimental method, the product samples' EDTA-Co bond were determined depending on the initial EDTA and EDTA-Co material selection, and the P doping can be controlled depending on the presence or absence of triphenylphospine.

Sample Characterization Methods. The sample materials'morphology and porous structure was determined by field-emission scanning electron microscopy (FE-SEM, SIGMA, Carl Zeiss) and field-emission transmission electron microscopy (FE-TEM, JEM-F200) with an energy dispersive spectroscopy (EDS) detector. The crystal structures'EDTA-Co bonds were characterized via X-ray diffraction (XRD, Bruker-AXS) with a 2θ = 20º to 80º diffraction range. The diffractometer operated at 40 kV and was equipped with a Cu Kα radiation source.
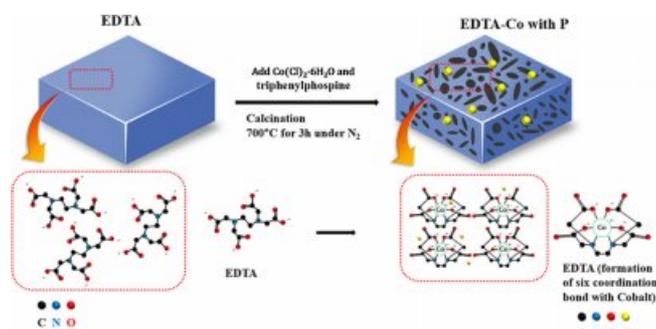

Schem 1. Fabrication process of EDTA-Co with P.

Electrochemical Property Measurements. Measurements of the electrocatalytic (Produced by the method shown in Schem 1) bifunctional properties (Oxygen Reduction Reaction - ORR & Oxygen Evolution Reaction - OER) and three-electrode mechanism system were carried out with a potentiostat (CH Instruments 600E, USA) and a rotating-disk electrode (RDE). Platinum wire (counter electrode), Ag/AgCl electrode (reference electrode), and a glassy carbon electrode (GCE, diameter: 5.0 mm, working electrode) were used for taking measurements. Prior to the measurements, the GCE surface was cleaned on the polishing pad with 1 μm of polishing diamond and 0.05 μm of polishing alumina; then rinsed with DI water. Next, a catalytic ink (1000 μL mixture) was fabricated by adding 4.0 mg of powdered sample to 5% Nafion solution, isopropanol, and DI water in a solution volume ratio = 1:3:6. After sonication for 1 h, 7 μL of ink was dropped onto the GCE surface and allowed to dry for 40 min at 40 °C. 0.1 M KOH electrolyte was purged with oxygen and nitrogen for 1 h and then the bifunctional test was performed. The bifunctional properties of electrocatalytic activity were evaluated by linear sweep voltammetry (LSV) and cyclic voltammetry (CV) at 10 mV/s of scan rate in a voltage range from 0.2 to -1.0 V (ORR with O_2 sat) and 0.2 to 1.0 V (OER with N_2 sat) with rotation speeds from 1600 rpm.

Results and Discussion

The electrocatalytic samples' porous properties and the morphological structure of EDTA with Co and P were examined via FE-SEM. In this study, EDTA was used as the main base-carbon material, to which a suitable amount of Co and P were added. The carbon-based material has high stability and durability, but it improves reactivity by doping hetero atom to improve the disadvantage of low reactivity with oxygen. N is the most widely used hetero atom, but in this study, P was used to induce synergistic effects with cobalt. Phosphorus is located in the same group as nitrogen and has as much charge as nitrogen, so it is expected to increase the reactivity with oxygen by redistributing charge when doping carbon material. In addition, when Co and P co-doping, the spin density and charge energy density on the catalyst surface change, leading to more positive effects than simply adding the effects of cobalt and P, respectively.

Figure 1(a) depicts low magnification SEM images of EDTA, which shows carbon planks similar to a plate. However, when combined with Co, EDTA exhibits a porous
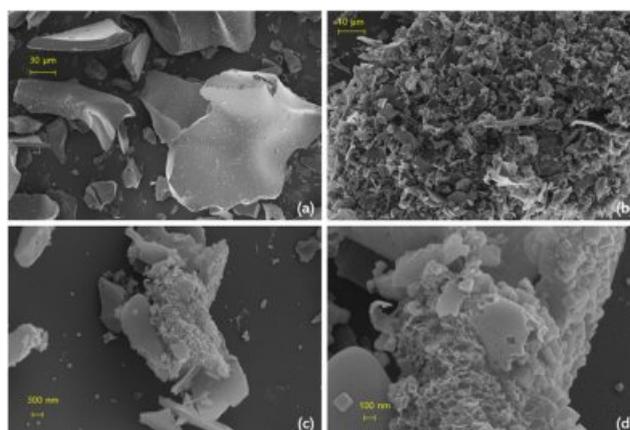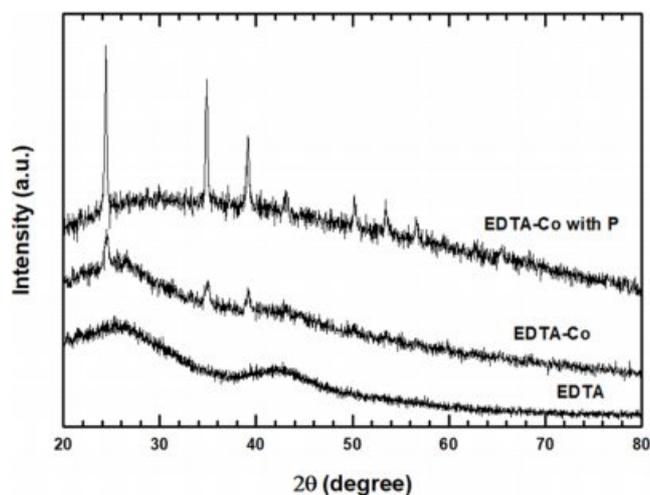
Figure 1. FE-SEM images of (a) low-magnification EDTA; (b) EDTA-Co; (c) and (d) high-magnification EDTA-Co with P.
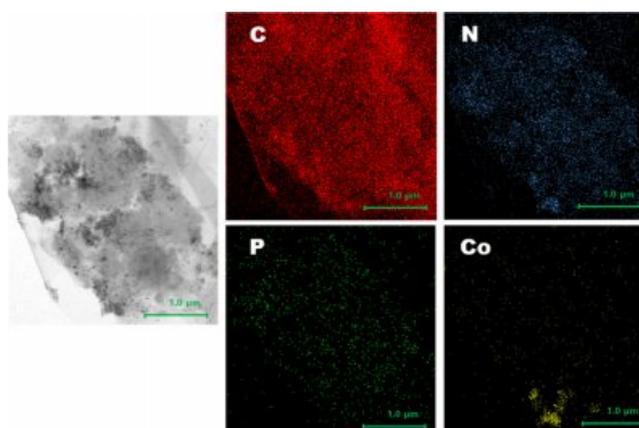
Figure 2. EDS mapping images (element of C, N, P, Co) by FE-SEM.

appearance (see Figure 1(b)). EDTA interacts with the transition metal to form six coordination bonds; it also exhibits an octahedral structure. Throughout this process, EDTA maintains a porous texture and develops a wider specific surface area. Figure 1(c) and 1(d) are high magnification images of P doped EDTA-Co. Note the rough surface and porous structure, which indicates that the Co and P particles were cultivated next to carbon's porous structure. In addition, the high magnification SEM image shows pore sizes in the micropore range, i.e., ≤ 2.0 nm

The electrocatalytic samples' EDS mapping image (in Figure 2) shows that the C, N, P and Co elements are grown in high concentrations. Because the primary material is carbon-based, carbon's EDS mapping range is the most clear and distinct. In addition, the image confirms that P is uniformly dispersed throughout the material, which demonstrates that P can
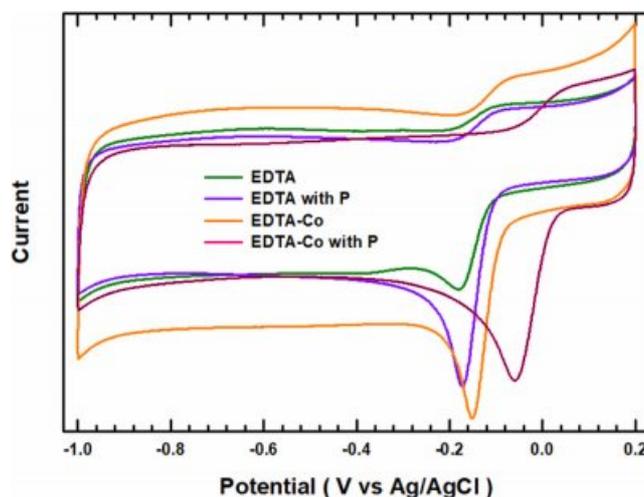
Figure 3. XRD patterns of EDTA, EDTA-Co and EDTA-Co with P catalyst.

Figure 4. Cyclic voltammetric profile for electrochemical catalyst in O_2-saturated 0.1 M KOH electrolyte at scan rate of 10 mV s^{-1}.

facilitate the C and Co bonding process. The EDS mapping image also depicted cultivation of Co particles, indicating that the amount of Co particles was contained. These results demonstrate that the cathode catalytic samples were successfully synthesized.

In Figure 3, the XRD pattern was acquired to confirm the morphology and formation/extent of EDTA-Co bonding. Various diffraction peaks were identified, including C and Co, and an amorphous characteristic. The $2\theta = 24^{\circ}$ peak with most pronounced crystallinity is a reflection of the original carbon phases.[16] Furthermore, the intensity and width of the diffraction peaks increase with increasing Co and P content. In addition, the peak at 35° verifies the formation of an orthorhombic phase perovskite-like structure.[17] The peak at 39° is a Co related peak. As P is added, the peak is incresed, indicating that P adds a synergistic effect to the binding of EDTA and Co.[18]

Materials comprised of EDTA-Co supplemented with P have a high electrocatalytic activity performance, e.g., ORR and OER, owing to their large surface area and the combination of P and Co elements enhancing the synergy effect of the C graphitic properties. Electrochemical measurements (CV, ORR, and OER) of the samples were evaluated via the RDE method using a typical three-electrode system. ORR and OER experiments on the cathodic catalyst samples and Pt/C material were performed by immersing them in O_2 and N_2 saturated 0.1 M KOH and taking RDE measurements at 1600 rpm and a 10 mV/s scan rate to confirm the electrochemical characteristics of the catalysts. Cyclic voltammetry (CV) curves (see Figure 4) focused on the oxygen reduction peak of the samples

and Pt/C material in a voltage range from -1.0 to 0.2 V (*vs*. Ag/AgCl). The corresponding CV curve exhibits reversible characteristics that enables both charge and discharge. Catalysts not containing Co and P show a very weak reaction peak and low onset potential (-0.185 V). The peak intensity increases as the amount of additive Co, P and Co with P increases, and the onset potential gradually increases (faster) as well (EDTA: -0.185 V, EDTA with P: -0.173 V, EDTA-Co: -0.152 V, EDTA-Co with P: -0.059 V).

The LSV curve also demonstrates the enhancement in electrochemical properties with the addition of Co and P. The electrocatalytic performance was obtained by RDE measurement at 1600 rpm and 10 mV/s of scan rate using oxygen saturated 0.1 M KOH solution. Analysis of the LSV curve in Figure 5 shows that the onset potential and the half-wave potential of EDTA-based materials and P-containing EDTA materials are almost identical (E_{onset}: -0.123 V, $E_{half-wave}$: -0.178 V). P shows that charge redistribution occurs due to changes in charge density and spin density, and the current density is higher as compared to the EDTA material alone (-4.12 to -4.58 mA/cm^2). Co exhibited a greater synergistic effect with EDTA material than P (E_{onset}: -0.105 V, $E_{half-wave}$: -0.163 V). Co has an octahedral structure and six coordination bonds with EDTA, as well as a high surface area, both of which lead to high performance in an electrochemical catalyst. A material in which Co and P are jointly added has more than just two effects (E_{onset}: -0.087 V, $E_{half-wave}$: -0.149 V). These results are caused by the P charge redistribution effect and the high specific surface area through the six EDTA-Co coordination bonds.
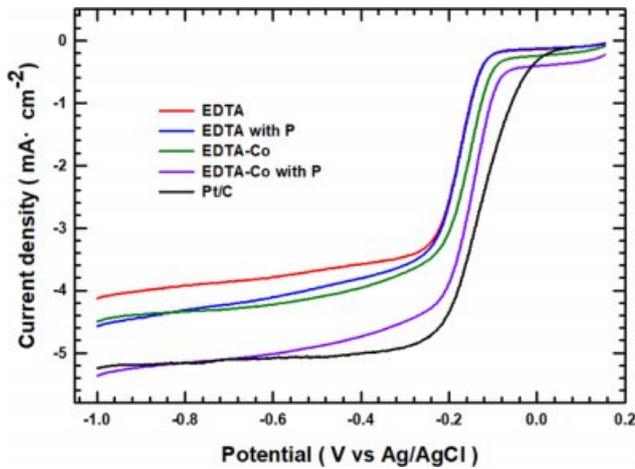
Figure 5. LSV curves (ORR) of EDTA, EDTA with P, EDTA-Co, EDTA-Co with P and Pt/C at rotating speed of 1600 rpm with O_2 saturated 0.1 M KOH media.
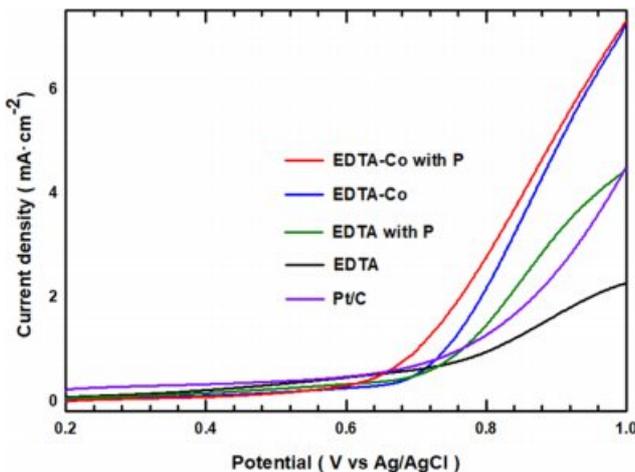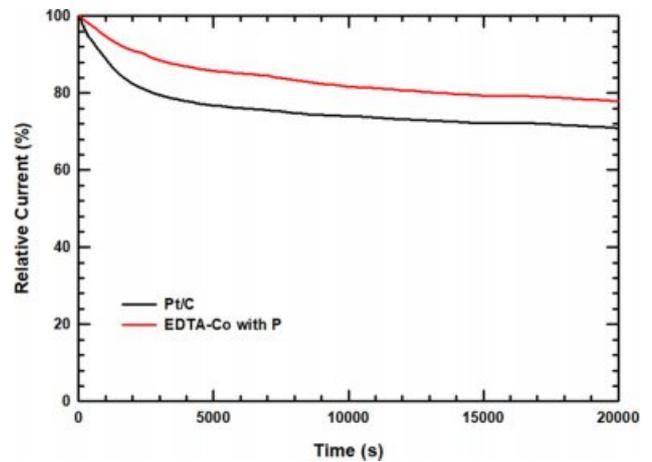

Figure 6. LSV curve (OER) of EDTA, EDTA with P, EDTA-Co and EDTA-Co with P at rotating speed of 1600 rpm with N_2 saturated 0.1 M KOH electrolyte.

The OER curve showing the electrochemical catalyst characteristics with ORR is shown in Figure 6. The RDE was measured using a rotating speed of 1600 rpm and a scan rate of 10 mV/s with nitrogen saturated 0.1 M KOH solution. The results are in good agreement with the CV and LSV curves, and shows that the performance increases with the addition of P and Co in OER activities. Only EDTA (0.748 V), EDTA with P (0.676 V), EDTA-Co (0.662 V) and EDTA-Co with P (0.607 V) show an increase in onset potential. Furthermore, with the exception of only EDTA material, the samples show higher onset potential than Pt/C (0.683 V), which is itself an excellent electrochemical catalyst. In addition, the catalytic

Table 1. Comparison of OER Catalytic Performance for EDTA, EDTA with P, EDTA-Co, EDTA-Co with P and Pt/C

Catalysts	E_{onset} (V) (V *vs*. Ag/ AgCl)	E_{OER} (V)/ J=4 mAcm^{-2} (V *vs*. Ag/AgCl)	Limited current density (mAcm^{-2})
EDTA	0.7834	-	2.266
EDTA with P	0.7122	0.9661	4.409
EDTA-Co	0.6784	0.8725	7.215
EDTA-Co with P	0.5982	0.8533	7.306
Pt/C	0.7902	0.9787	4.498

Figure 7. Relative current density of EDTA-Co with P and Pt/C catalyst for 20000 s at -0.6 V.

samples reached a current density of 4 mA/cm^2 at a faster potential than Pt/C (see Table 1). Table 1 compares the samples' electrochemical properties (OER) and those of Pt/C. Thus, through the above-mentioned electrochemical experiments, we confirmed the positive effect P and Co individually contribute, and demonstrated the development of a successful electrochemical catalyst based on a superior synergistic effect when P and Co are simultaneously added.

In this work, these changes were evaluated using a chrono-amperometric approach where measurements were performed at -0.6 V for 20000 s in an O_2 saturated 0.1 M KOH media in Figure 7. Pt/C shows a sharp drop in the initial stage of operation, and then decreases steadily, demonstrating that decreases by 70.3%. However, EDTA-Co with P electrocatalyst has no rapid drop in relative current and shows high durability of 78.8% after running for 20000 s.

Conclusions

In this work, we successfully demonstrated the synergistic

effect of coupling between P, Co and EDTA. The six ligand sites of EDTA bind to the transition metal with coordinate bonding and form an octahedral structure. In addition, the P particle is located between Co and EDTA bond, triggering atomic and spin charge density changes that result in charge redistribution on the catalyst's surface. This process changes the chemical adsorption energy of O_2, and therefore affects the material much more so than simple Co and P doping. P-doped EDTA and Co structures were verified by FE-SEM and FE-TEM and further confirmed by XRD analysis. The location of EDTA-Co with P of electrochemical properties was measured by chronoamperometry and potentiostat methods. CV and LSV curves confirmed that P and Co samples had a synergistic effect on the electrochemical.

References

1. B. C. Steele and A. Heinzel, in *Materials For Sustainable Energy, A Collection of Peer-Reviewed Research and Review Articles from Nature Publishing Group*, World Scientific, pp. 224-231 (2011).

2. A. Rabis, P. Rodriguez, and T. J. Schmidt, *ACS Catal.*, **2**, 864 (2012).

3. Y. Bing, H. Liu, L. Zhang, D. Ghosh, and J. Zhang, *Chem. Soc. Rev.*, **39**, 2184 (2010).

4. X. Wang, J. S. Lee, Q. Zhu, J. Liu, Y. Wang, and S. Dai, *Chem. Mater.*, **22**, 2178 (2010).

5. J. S. Lee, S. T. Kim, R. Cao, N. S. Choi, M. Liu, K. T. Lee, and J. Cho, *Adv. Energy Mater.*, **1**, 34 (2011).

6. E. M. Erickson, M. S. Thorum, R. Vasić, N. A. S. Marinković, A. I. Frenkel, A. A. Gewirth, and R. G. Nuzzo, *J. Am. Chem. Soc.*, **134**, 197 (2011).

7. J. Zhang and L. Dai, *ACS Catal.*, **5**, 7244 (2015).

8. L.-y. Feng, Y.-j. Liu, and J.-x. Zhao, *J. Power Sources*, **287**, 431 (2015).

9. Q. Liu, S. Chen, Y. Zhou, S. Zheng, H. Hou, and F. Zhao, *J. Power Sources*, **261**, 245 (2014).

10. Z. Yang, Z. Yao, G. Li, G. Fang, H. Nie, Z. Liu, X. Zhou, X. A. Chen, and S. Huang, *ACS Nano*, **6**, 205 (2011).

11. X. Solans, M. Font-Altaba, J. Oliva, and J. Herrera, *Acta Crystallogr. Sect. C: Cryst. Struct. Commun.*, **39**, 435 (1983).

12. Z. Liu, G. Zhang, Z. Lu, X. Jin, Z. Chang, and X. Sun, *Nano Res.*, **6**, 293 (2013).

13. H.-W. Liang, W. Wei, Z.-S. Wu, X. Feng, and K. Müllen, *J. Am. Chem. Soc.*, **135**, 16002 (2013).

14. J. Wu, C. Jin, Z. Yang, J. Tian, and R. Yang, *Carbon*, **82**, 562 (2015).

15. S. Jiang, C. Zhu, and S. Dong, *J. Mater. Chem. A*, **1**, 3593 (2013).

16. R. Li, Z. Wei, and X. Gou, *ACS Catal.*, **5**, 4133 (2015).

17. B. Zhang, M. Pan, D. Zhao, and W. Wang, *Appl. Phy. Lett.*, **85**, 61 (2004).

18. J. Wu, Z. Yang, X. Li, Q. Sun, C. Jin, P. Strasser, and R. Yang, *J. Mater. Chem. A*, **1**, 9889 (2013).